STRAIN ESTIMATION USING A MODAL EXPANSION APPROACH VIA VIRTUAL SENSING FOR STRUCTURAL ASSET MANAGEMENT

C. Roberts, S. Isbister, C. Murphy, C. Nisbet, P. Sweeney, **D. Garcia**, University of Strathclyde, UK
D. Tcherniak, *Bruel & Kjaer Sound & Vibration Measurement, Denmark*

ABSTRACT

This study explores the concept of virtual sensing as a potential application for estimating dynamic strain in a virtual location. The study was carried out on a vertical cantilever beam which was used to represent a vertical structure. The acceleration responses were measured in four locations and, through Operational Modal Analysis (OMA) and Modal Decomposition and Expansion (MDE) techniques, was then estimated in a virtual location. The dynamic strain was then estimated in the same virtual location.

First the measured acceleration responses were compared to predicted responses using OMA. This was done to update the finite element model and optimise the position of the sensors. From this point the dynamic strain could then be estimated in the virtual location using Modal Decomposition and Expansion. This methodology was then repeated for the same beam with additional mass attached to the top. The dynamic strains were then measured and compared to determine the effect of the additional mass on the structural response.

The results from this study demonstrated the potential of this methodology to estimate and monitor real time dynamic strain in virtual locations.

1. INTRODUCTION

Structural health monitoring (SHM) is primarily used to monitor the condition of a structure as, over the long service life of an asset, deterioration of the structure will inevitably occur due to a large range of factors. These can range from environmental corrosion, operational variation and fatigue. Offshore structures, such as wind turbines, are extremely prone to fatigue failure due to the large number of stress cycles from wind, waves and operation [1]. SHM can be used to identify the effects of fatigue, meaning it can be an extremely useful tool for assessing asset integrity and, ultimately, prolonging and optimising asset production. SHM consists of four main stages: operational evaluation, data acquisition, feature selection and finally decision making [2].

There are countless benefits to SHM and it is currently a massively growing research area. One of the main benefits is that it allows for continuous, real time monitoring meaning damage to a structure can be identified early. This can be used to minimise downtime and optimise maintenance strategies [3]. Cost studies [4] show that the operation and maintenance costs for offshore assets is accountable for almost a quarter of the overall asset cost. It is not restricted to new assets and can be implemented on existing structures; thus, it can be beneficial to existing operators.

1.1 VIRTUAL SENSING

Virtual sensing allows for the estimation of kinetic and mechanical parameters at locations where there are no sensors placed [5]. This is particularly useful for offshore assets such as oil platforms and wind turbines where there are areas of high stress in the subsea components. These areas would be extremely difficult, or impossible, to place a sensor meaning virtual sensing would be necessary to estimate the levels of stress or strain at these locations. This is a powerful tool and can provide a real insight into operation conditions of critical subsea components. There are a number of methods used to apply virtual sensing.

There are many advantages to the implementation of virtual sensing. One of the main and obvious advantages is that it can be used to prevent critical shutdowns by estimating the stresses and strains and therefore the time to failure of components. This reduces costs by optimising maintenance and inspection whilst also reducing the downtime of the asset. Another benefit is that any location on the asset can be monitored without having to physically place a senor in that location [6]. The installation of a sensor may be a complicated job depending on the location, so having the ability to virtually monitor this area would be hugely beneficial.

This paper combines Operational Modal Analysis (OMA) and modal decomposition and expansion to estimate dynamic strain at a virtual location. The overall aim of this project was to conclude on the feasibility of this method and propose how it could be implemented in industry. In order to achieve this, a measurement rig was required that would be used for conducting experimental work as well as a simple finite element model of the structure. Once the model and rig had been created the experiment was then conducted. By using the obtained modal parameters, the finite element model was updated for good agreement of mode shapes and Modal Assurance Criterion (MAC) value. From this stage the strain could be estimated using the methodology and the results could be validated by values obtained from placed accelerometers and strain gauges. Once the strain values had been validated the experiment would then be repeated with additional mass to determine the changes to the structural response. A conclusion on the feasibility would then be made by assessing the usability of the method with its advantages and drawbacks as well as a proposal on how the method could be used in industry.

2. METHODOLOGY

The methodology used in this study is outlined in figure 1 below. Each step will be explained in further detail during this report.

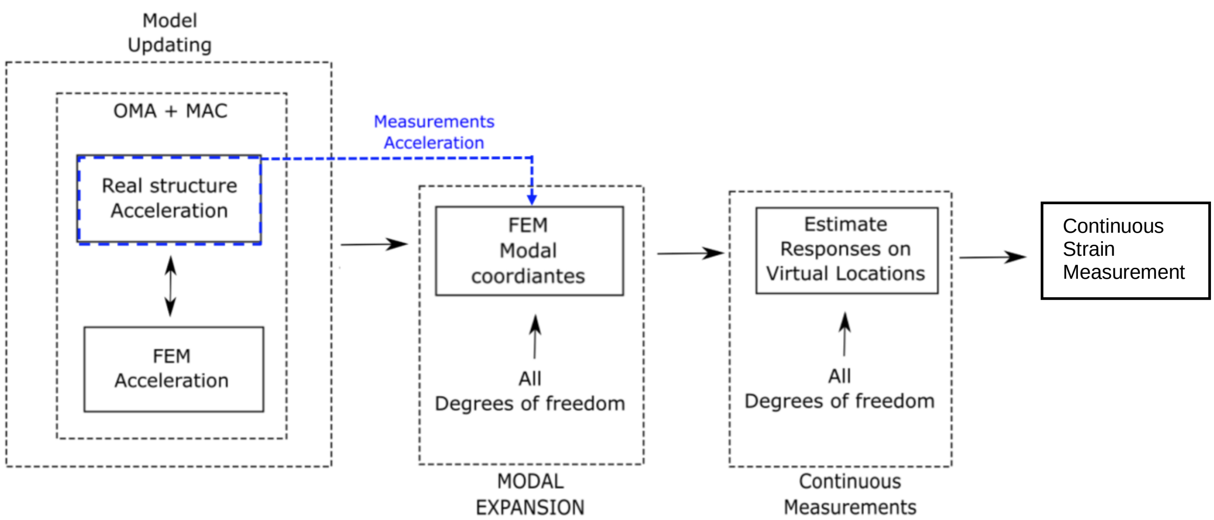

Figure 1: Methodology flow chart

2.1 OPERATIONAL MODAL ANALYSIS

Operational modal analysis (OMA) was used to determine the modal parameters of the test specimen. For this study, the acceleration mode shapes were compared for both real and simulated systems in order to update the simulated system. This was essential to accurately predict the strain at virtual locations.

To quantitatively determine the quality of the correlation between the experiment and the finite element model, the modal assurance criterion (MAC) was used. The MAC number, equation 1, compares the acceleration mode shape from the real and simulated system and has a maximum value of one, signifying perfect correlation. The position of the accelerometers can also be optimised using a MAC study [7].

$$MAC_{ij} = \frac{\left|\emptyset_i^T\ \emptyset_j\right|^2}{(\emptyset_i^T\ \emptyset_i)\ (\emptyset_j^T\ \emptyset_j)} \qquad \textbf{(1)}$$

In addition to the correlation of mode shapes between the finite element model and test specimen, the placement of accelerometers along the cantilever beam is also very important for the quality of results. There is an optimum placement of sensors which will provide an orthogonal matrix for the MAC values. For example, it is required that the diagonal of the resultant MAC matrix is as close to 1 as possible, however simultaneously the off-diagonal values should have low MAC values to ensure good orthogonality. If the MAC values of the off-diagonal terms are not reduced, this will affect equation 7 making it sensitive to errors in the mode shapes and therefore affecting future strain results [8]. This demonstrates that an optimum placement of sensors is essential to ensure orthogonality and obtain more accurate results for further calculations.

2.2 MODAL DECOMPOSITION

Consider a model of a vibrational system, with no damping which is described by the equation of motion for a structure subjected to an external force f(t):

$$M\boldsymbol{a}(\boldsymbol{t}) + K\boldsymbol{x}(\boldsymbol{t}) = \boldsymbol{f}(\boldsymbol{t}) \qquad \textbf{(2)}$$

Where **M** is the mass matrix, **K** is the stiffness matrix, $\boldsymbol{a}(\boldsymbol{t})$ is the acceleration vector, $\boldsymbol{x}(\boldsymbol{t})$ is the displacement vector and $\boldsymbol{f}(\boldsymbol{t})$ is the force vector.

The eigenvalue equation for this system may be expressed as:

$$\omega^2 M\boldsymbol{\varphi_i} = K\boldsymbol{\varphi_i} \qquad \textbf{(3)}$$

The eigenvalues are represented by $\lambda = \omega^2$ and the mode shape vectors $\boldsymbol{\varphi_i}$**.** The displacement vector of the system can be represented as a linear combination of the mode shape vectors:

$$\boldsymbol{x}(\boldsymbol{t}) = \sum_{\boldsymbol{i=1}}^{\boldsymbol{n}} \boldsymbol{\varphi_i q_i}(t) \qquad \textbf{(4)}$$

Writing the above equation in matrix form

$$\begin{aligned} &\boldsymbol{x}(\boldsymbol{t}) = \emptyset \boldsymbol{q_i}(t) \\ &\emptyset = [\boldsymbol{\varphi_1}\ \boldsymbol{\varphi_2}\ \boldsymbol{\varphi_3} \cdots \boldsymbol{\varphi_n}] \qquad \textbf{(5)} \\ &\boldsymbol{q_i}(t) = [\boldsymbol{q_1}(t)\ \boldsymbol{q_2}(t)\ \ldots\ \boldsymbol{q_n}(t)]^T \end{aligned}$$

Where $\boldsymbol{q_i}(t)$ is the modal coordinates vector for each time (t) which hold details of the few mode shapes that contribute most to the vibrational response of the system. Φ is the mode shape matrix and n is the total number of modes.

2.3 MODAL EXPANSION

Modal expansion takes the estimated modal displacements, obtained from section 2.1 and uses them to calculate output quantities at the virtual sensor locations.

An expression for the limited number of experimentally measured displacements, at known locations, may be determined using a similar equation as in the modal decomposition methodology:

$$\boldsymbol{x_m}(\boldsymbol{t}) = \emptyset_{\boldsymbol{m}} \boldsymbol{q}(t) \qquad \textbf{(6)}$$

Where the subscript m refers to the measured degree of freedoms.

The modal co-ordinates of the system may then be determined using a pseudo inverse:

$$\boldsymbol{q}(\boldsymbol{t}) = (\emptyset_{\boldsymbol{m}}^{\boldsymbol{T}} \emptyset_{\boldsymbol{m}})^{-1} \emptyset_{\boldsymbol{m}}^{\boldsymbol{T}} \boldsymbol{x_m}(t) \qquad \textbf{(7)}$$

This result is then expanded to obtain the displacements at the virtual locations (subscript *v* refers to the virtual DOF's):

$$\begin{aligned} \boldsymbol{x_v}(\boldsymbol{t}) &= \emptyset_{\boldsymbol{v}} \boldsymbol{q}(t) \\ &= \emptyset_v (\emptyset_{\boldsymbol{m}}^{\boldsymbol{T}} \emptyset_{\boldsymbol{m}})^{-1} \emptyset_{\boldsymbol{m}}^{\boldsymbol{T}} \boldsymbol{x_m}(t) \end{aligned} \qquad \textbf{(8)}$$

2.4 PREDICTED ACCELERATIONS

Similarly, the accelerations may be determined by the same Modal Decomposition and Expansion (MDE) approach described in the previous sections:

$$\boldsymbol{a_m}(\boldsymbol{t}) = \emptyset_{\boldsymbol{m}} \boldsymbol{q_a}(t) \qquad \textbf{(9)}$$

Where $\boldsymbol{q_a}(t)$ describes the acceleration modal co-ordinates for time instant t. The acceleration modal co-ordinates of the system may then be determined using a pseudo inverse [9].

$$\boldsymbol{q_a}(t) = (\emptyset_{\boldsymbol{m}}^{\boldsymbol{T}} \emptyset_{\boldsymbol{m}})^{-1} \emptyset_m^T \boldsymbol{a_m}(t) \qquad \textbf{(10)}$$

This result is then expanded to obtain the accelerations at the virtual locations:

$$\begin{aligned} a_v(t) &= \emptyset_v \boldsymbol{q_a}(t) \\ &= \emptyset_v (\emptyset_{\boldsymbol{m}}^{\boldsymbol{T}} \emptyset_{\boldsymbol{m}})^{-1} \emptyset_{\boldsymbol{m}}^{\boldsymbol{T}} \boldsymbol{a_m}(t) \end{aligned} \qquad \textbf{(11)}$$

2.5 STRAIN ESTIMATION

A significant part of the research for this project is to determine a value of strain at an unknown location on the cantilever beam. Therefore, the strain at each time may be found using the following equation:

$$\begin{aligned} &\varepsilon(t, x, mode) \\ &= \emptyset_\varepsilon \mathcal{F}^{-1} \left(\frac{1}{-\omega^2} \mathcal{F} \left(\emptyset^\dagger a(t, x) \right) \right) \end{aligned} \qquad \textbf{(12)}$$

Each of the individual mode shape responses may be summed to determine the global response of the system in the following way:

$$\begin{aligned} &\boldsymbol{x}(t)_{global} \\ &= \sum \boldsymbol{x}(t)_{mode\,1} \\ &+ \boldsymbol{x}(t)_{mode\,2} + \cdots \end{aligned} \qquad \textbf{(13)}$$

To convert to strain as opposed to a displacement, the displacement is multiplied by the peak strain as a result of each mode shape:

$$\begin{aligned} &\varepsilon(t, mode) = [\emptyset]_\varepsilon [\boldsymbol{q}(t)] \\ &= \begin{bmatrix} x_1 \\ x_2 \\ x_3 \\ x_4 \end{bmatrix} [\boldsymbol{q}(t_1) \quad \boldsymbol{q}(t_2) \quad \boldsymbol{q}(t_3) \quad \boldsymbol{q}(t_4)] \end{aligned} \qquad \textbf{(14)}$$

Where,

$$[\emptyset]_\varepsilon = \varepsilon_{max} \begin{bmatrix} x_1 \\ x_2 \\ x_3 \\ x_4 \end{bmatrix} \qquad \textbf{(15)}$$

ε_{max} is the peak strain identified at the discretised location found using the FEA simulation. These values may then be summed, as before, to determine the overall strain for the system.

$$\begin{aligned} \varepsilon(t)_{global} = \sum &\varepsilon(t)_{mode\,1} \\ &+ \varepsilon(t)_{mode\,2} \\ &+ \cdots \end{aligned} \qquad \textbf{(16)}$$

2.6 EXPERIMENTAL SYSTEM

In order to conduct OMA and conclude on the usability, an experimental system was required. The experiment made use of five accelerometers, four sensors and one for verification in the virtual location, which were secured to a vertical aluminium cantilever beam in the configuration shown in figure 2. These accelerometers fed into a front end which transferred the data from the sensors to the software where the data could be processed and interpreted. This stage provided mode shapes and natural frequencies of the beam which could be used to optimise and refine the finite element model. The data was then exported into MATLAB where it was interpreted completely.

This methodology could be applied to a real-world structure to conduct SHM. In order to do this an accurate FEA model would be required which, depending on the complexity of the structure, may be a challenge. In order to accurately measure the structural response, a large number of accelerometers may be required which would increase the complexity of the OMA and sensor placement optimisation. Once this was complete the data from the sensors would feed into the processing and interpretation software to provide the real-time dynamic strain response of the structure.

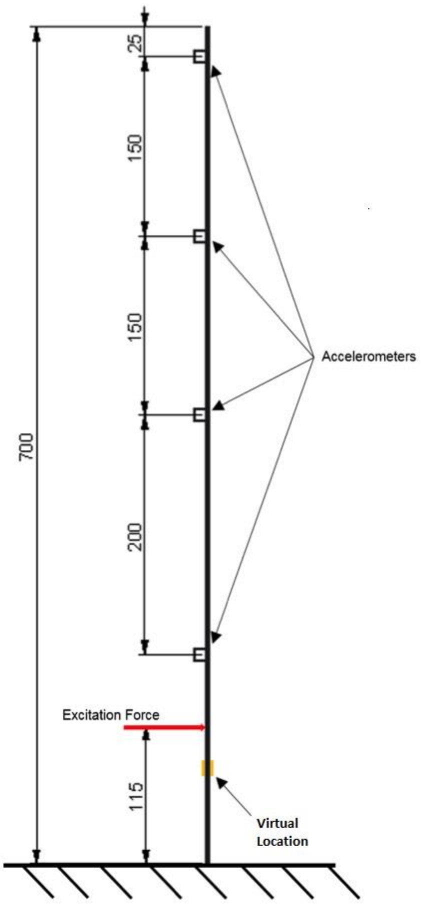

Figure 2: Schematic of experimental setup

If this methodology was applied it would provide a great insight into the accelerations and strains of the structure in areas which would be difficult or impossible to place a sensor. This data could be used by engineers to better understand the operating conditions of the asset in hard to reach areas.

3. BEAM DESIGN

3.1 DESIGN CRITERIA

For the experiment to be effective, the beam had to be designed carefully to ensure the best possible results.

The beam was designed to be a rectangular cantilever and so that it vibrates with one dominant set of modes, which in this case was flap. It was chosen that the beam should be made from a low cost metal and that the first natural frequency should exist between 5 and 10 Hertz. Finally, the ideal scenario should be that the first of the other vibration types should be outside the first four flap frequencies.

3.2 ANALYSIS OF VIBRATION TYPES

Table 1, shown below, displays the first four modes for each vibration type for the beam dimensions used in this investigation (700x50x3)mm. This particular case fails the ideal scenario as the first edgewise mode is between the second and third transverse (flap) modes and the first torsional exists between the third and fourth transverse modes.

Table 1: Natural frequencies for first four modes

Mode Number	Flap (Hz)	Edge-wise (Hz)	Torsi-onal (Hz)	Longit udinal (Hz)
1	5.07	84.52	132.6	285.7
2	31.7	529.7	399.2	857.0
3	88.9	1482	669.1	1428
4	174.4	2906	944.8	1999

It was found that the ideal scenario could not be achieved. A compromise was reached such that these were the only two modes that existed in the range. The mode was to be distinct from both such that a transverse and torsional mode could not be simultaneously excited.

3.3 FINAL DESIGN

The final geometry of the beam was (750x50x3)mm. When modelling the beam the dimensions of (700x50x3)mm were used as 50mm of the beam was to be clamped in the test rig. The beam was manufactured from aluminium sheet.

4. RIG DESIGN

The rig was designed in order to meet a set of criteria. These criteria included: the rig must hold the test specimen in a vertical orientation, the rig must clamp the test specimen at the base without any possibility of movement in a vertical or horizontal orientation and the rig must be stable under its own weight.

The base of the rig is a square section with a major dimension of 600mm and is designed to sit flat on the floor.

The test specimen was clamped vertically between two sections of steel with two bolts through the test specimen to prevent rotation.

The rig must have the facilities to hold a shaker, used to excite the test specimen. The shelf was also made to be adjustable so that the force could be applied at different points on the test specimen.

The resulting experimental rig design complied with the all design criteria. Figure 3 shows the final design.

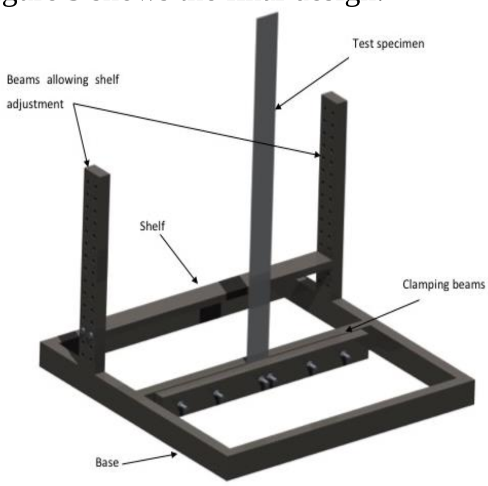

Figure 3: 3D model of experimental rig with test specimen

5. RESULTS AND DISCUSSION

5.1 OPERATIONAL MODAL ANALYSIS

Normalised mode shapes for the first four modes were obtained experimentally using the method described previously as well as taken from the updated finite element model. A comparison of the shapes is shown in figures 4(a)-(d). A visual inspection of the results reveals a qualitatively high degree of similarity between the theoretical and measured modes. This suggests that the finite element model accurately represents the real system for the first four flap modes.

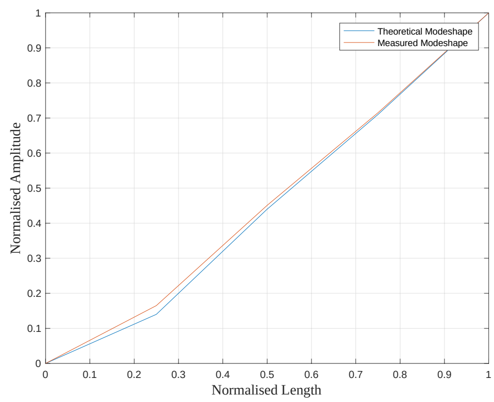

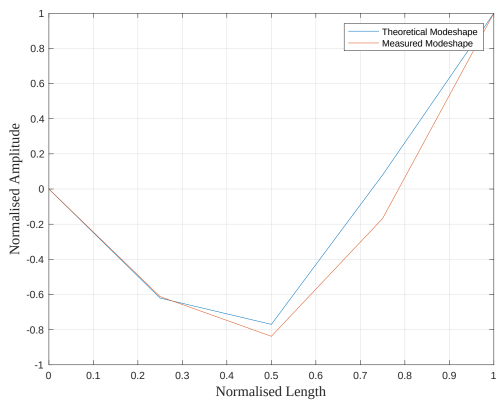

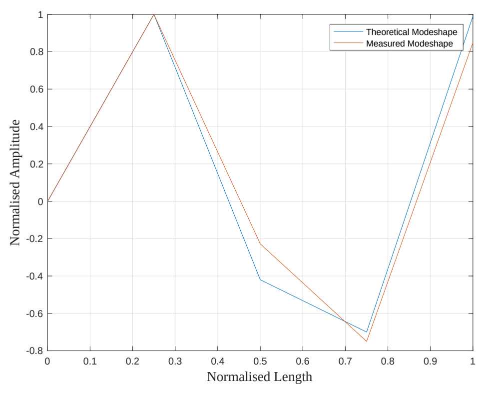

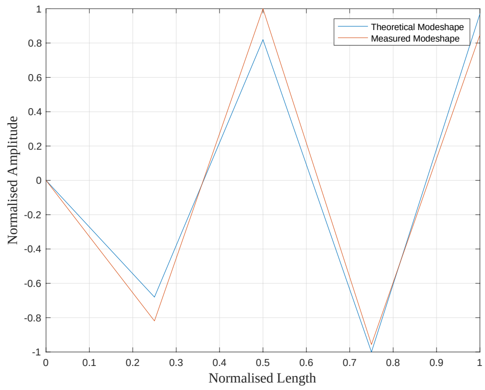

Figure 4: Theoretical vs measured mode shapes. 4a - 1st mode shape, 4b - 2nd mode shape, 4c - 3rd mode shape, 4d - 4th mode shape

The modal assurance criterion gives a quantitative overview of the accuracy of the finite element model. Using equation from section 2.1, it is possible to determine the sixteen corresponding MAC numbers. Figure 5 shows the array of MAC numbers obtained from the final iteration of the method.

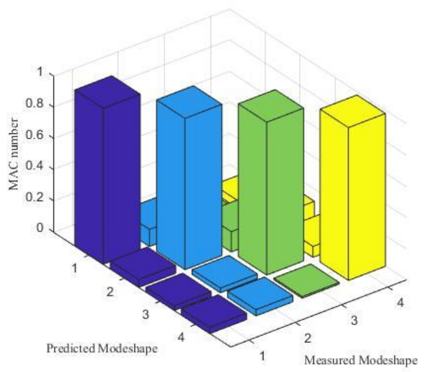

Figure 5: MAC study results

For this type of analysis, it is important for the main diagonal to be as high as possible and the off-diagonals to be as low as possible. The results from this study contain a main diagonal with a minimum value of 0.97 and maximum off-diagonal value of 0.13. These results prove that there is an elevated level of correlation between the finite element model and the experimental test specimen. Therefore, by using the mode shapes obtained from the finite element model and the position of the virtual location, it will be possible to predict the acceleration, and thus strain, at the virtual location using the other accelerometers with a high degree of accuracy.

With a large investment of time, it could be possible to improve the quality of these results. For the application of this methodology on real structures, this increase of quality would be necessary. However, for the purposes of proving the methodology, the correlation between the finite element model and real system is sufficient. An increase would be unlikely to have a significant impact on the overall results.

5.2 ACCELERATION COMPARISON

Figure 6 compares the measured and predicted acceleration signals, as predicted by the virtual sensing method. It is clear that whilst the instantaneous behaviours compare poorly, the global responses are comparable, indicating that a cycle counting method is reasonably practicable.

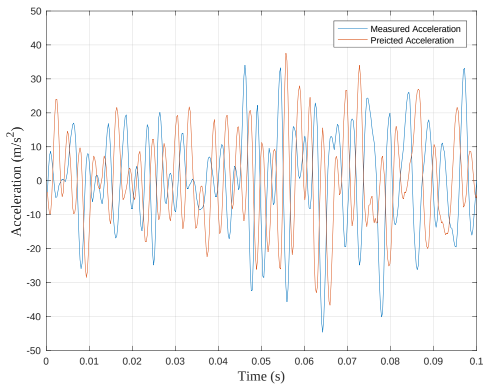

Figure 6: Measured and predicted (via virtual sensing acceleration Vs time for an arbitrary time period, showing global correlation

More compellingly, the normalised spectral densities, figure 7, show similar values, with each of the first four modes predicted to an accuracy of at least two significant figures (provided in section 5.5).

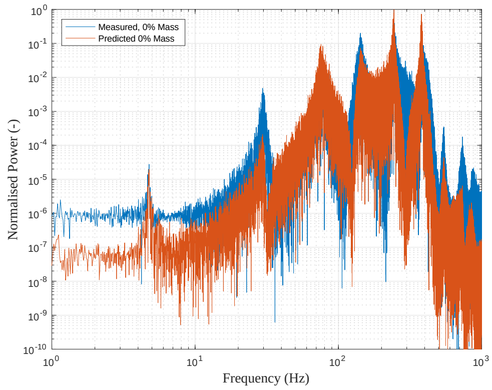

Figure 7: Normalised frequency spectrum of the measured and predicted (via virtual sensing) acceleration at the virtual location

Modes beyond the first four have been identified by the methodology, and as such are predicted by the virtual sensing method however their relative is low compared to earlier modes because of the limitations of the sampling frequency used. There are also modes detected from other vibration types, in particular the first torsional mode (132.6Hz) is also clearly being predicted.

5.3 ACCELERATION COMPARISON WITH ADDITIONAL MASS

An additional tip mass was introduced in order to assess the systems capabilities under less idealised conditions. When an additional mass was added to the end of test specimen, the following power densities were observed, figure 8a with 5% of the mass of the beam added on the tip and figure 8b with 10% of the mass of the beam added on the tip.

The figures show a shift in the spectra compared to what would have been observed without the additional mass. This is the expected result as the natrual frequencies of a system are inversley related to the mass of the system. A small deviation in frequency is shown with a 5% additional tip mass and a greater deviation with a 10% tip mass. This demonstrates the systems sensitivity and capability to respond to small changes effectivley to monitor damage, as well as its robustness to work in atypical non-idalised conditions.

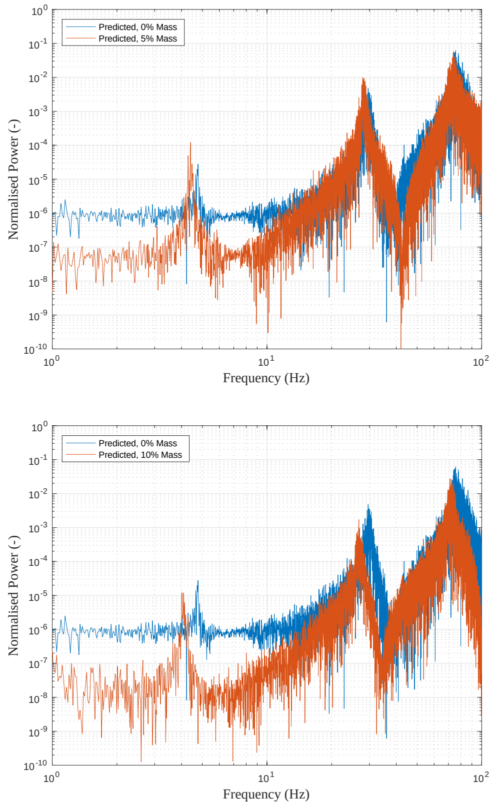

Figure 8: Normalised frequency spectrum of predicted (via virtual sensing) acceleration showing spectral shift with additional tip mass as measured at the virtual location. 8a - Tip mass of 5% compared with 0% tip mass, 8b - Tip mass of 10% compared with 0% tip mass

5.4 STRAIN COMPARISON

As outlined earlier in the paper, the goal of this methodology is to estimate dynamics strain, from global acceleration data in a virtual location. This has been carried out for both time series using Equation 12 and is shown below in figure 9a, additionally, the frequency series has been assessed as in figures 8a and 8b.

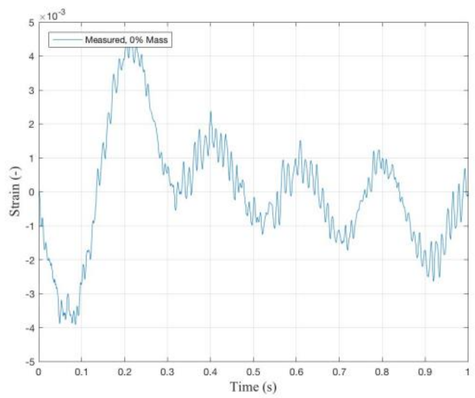

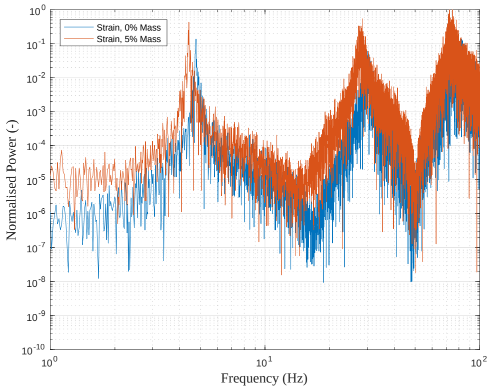

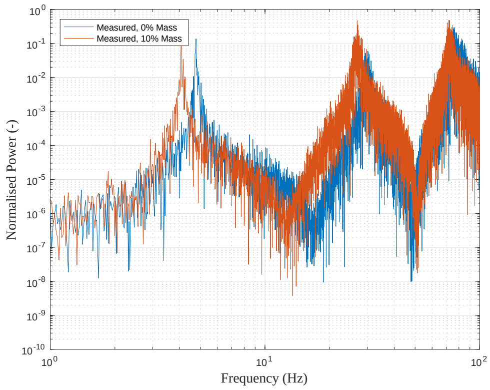

Figure 9: Behaviour of dynamic strain in the time and frequency domains as predicted (via virtual sensing) at the virtual location. 9a - strain Vs time for an arbitrary time period, 9b - Tip mass of 5% compared with 0% tip mass, 9c - Tip mass of 10% compared with 0% tip mass

It is interesting to note that the power densities of the strain compared to the acceleration are much more uniform, this is because the methodology used in modal expansion filters for expected mode shapes, and hence the natural modes in strain are closer to unity.

5.5 OVERALL

Shown below in tables 3 and 4, are the first 4 sequentially measured and predicted modes respectively, with modes 1-3 representing flap modes and the 4^{th} mode being the first torsional mode.

There is a slight deviation from the values of flap modes in Table 1, this is most likely due to a small change in Boundary Conditions (BC's) between experiments however the internal consistency between predicted and measured modes is extremely high and the deviation from the idealised model is inconsequential as this further demonstrates the applicability to real structures.

Table 3: Measured Modes

	1 (Hz)	2 (Hz)	3 (Hz)	4 (Hz)
0%	4.773	29.59	75.68	142.5
5%	4.408	27.91	74.00	135.0
10%	4.075	26.88	71.93	135.5

Table 4: Predicted Modes

	1 (Hz)	2 (Hz)	3 (Hz)	4 (Hz)
0%	4.773	29.62	75.68	142.5
5%	4.407	28.22	74.00	135.4
10%	4.008	26.78	71.19	135.0

6. CONCLUSION

From the results of this research, it is possible to conclude on the feasibility of the application of this methodology for a dynamic strain estimation in a virtual location and consequently to assess structural state condition. It was shown that it is possible to match, with a high degree of accuracy, the mode shapes of a real structure with ones predicted by a finite element model. However, the method that was applied to achieve this, change of position of the accelerometers, would be difficult to achieve on structures that are already in operation. Conversely, this method would be easier to apply to new structures through optimisation of accelerometer locations. Once optimised on one structure, it can then be applied to any new structure of the same design.

By adding an additional accelerometer in a virtual location to verify the results, it was proven that it is possible to predict the acceleration at any point on a structure. This section of the methodology has been verified and, therefore, could be applied to any real structure. However, the acceleration at a point is not the information that is important for structural health monitoring. The required value, and

the one that was aimed to be proved, was the strain. Due to incoherent data received from the strain gauge, it was not possible to prove that the strain, based on measured accelerations, can be predicted. In this respect, it is difficult to recommend on the feasibility of applying this methodology to real structures because of inconclusive results in this area.
Overall, the method for predicting strain set out in this report is still unverified and it would be dangerous to recommend applying it to real structures until it has been. However, it has been shown that the accelerations can be predicted, and this could be applied to real structures, providing the position of the accelerometers can be optimised. There is potential for new structures to be built with optimised sensor placement and then the methodology applied when it has been verified. However, this could be costly and time consuming if the methodology is never proved or if the technology becomes redundant due to new advances in the area.

ACKNOWLEDGEMENTS
The authors acknowledge the University of Strathclyde for the use of laboratory space and financial support. Furthermore, the authors acknowledge Brüel & Kjær for the use of their equipment.

REFERENCES
1. van der Male, P. and Lourens, E., 2015 ‘Estimation of accumulated fatigue damage in lattice support structures from operational vibrations’, In Proceedings of EWEA Offshore, Copenhagen, 2015.
2. Moreno-Gomez, A., Perez-Ramirez, C., Dominguez-Gonzalez, A., Valtierra-Rodriguez, M., Chavez-Alegria, O. and Amezquita-Sanchez, J., 2017 ‘Sensors Used in Structural Health Monitoring’. Archives of Computational Methods in Engineering, pp1-18
3. Fritzen, C., Kraemer, P. and Klinkov, M., 2011 ‘An Integrated SHM Approach for Offshore Wind Energy Plants’, Structural Dynamics, Volume 3, pp.727-740.
4. Delft University Wind Energy Research Institute (Duwind), 2001 ‘Concerted Action on Offshore Wind Energy in Europe’, Report Ref: Duwind 2001.006.
5. Lichuan Liu, Kuo, S. and Zhou, M., 2009 ‘Virtual sensing techniques and their applications’, 2009 International Conference on Networking, Sensing and Control.
6. Li, Haorong, Daihong Yu, and James E. Braun., 2011 ‘A Review of Virtual Sensing Technology and Application in Building Systems.’ HVAC&R Research 17 (5): 619–645.
7. Allemang R.J., 2003 ‘The Modal Assurance Criterion (MAC): Twenty years of Use and Abuse, Journal of Sound and Vibration’, 37(8); 14-21.
8. Iliopoulos A., 2017 ‘Virtual Sensing Techniques for Response Estimation and Fatigue Assessment of Offshore Wind Turbines’ [PhD]. Vrije Universitiet Brussel, pp 40-41.
9. Iliopoulos A, Shirzadeh R, Weijtjens W, Guillaume P, Hemelrijck D, Devriendt C., 2016 ‘A modal decomposition and expansion approach for prediction of dynamic responses on a monopile offshore wind turbine using a limited number of vibration sensors’ Mechanical Systems and Signal Processing, pp 2-3